Plasmonic hot carriers scratch the surface

Sushant Kumar,[1,*] Adela Habib[2,*] and Ravishankar Sundararaman[1,2,a]
[1]Department of Materials Science and Engineering, Rensselaer Polytechnic Institute,
[2]Department of Physics, Applied Physics and Astronomy, Rensselaer Polytechnic Institute
[*]These authors contributed equally. [a]sundar@rpi.edu
(Dated: August 2, 2021)

Metal nanostructures capture light efficiently due to plasmonic enhancement, and generate energetic electrons and holes that can be used to drive chemical reactions or transferred across metal-semiconductor interfaces for solar cells and photodetectors. The overall efficiency of plasmonic hot-carrier devices depends on the generated energy distribution, its evolution with transport through the metal, and most critically, on the transport across the metal surface or interface. Here, we review the mechanistic considerations, strategies and challenges for efficient hot carrier extraction, highlighting the need for new materials to transport carriers with minimal energy loss and for interfaces designed to transfer them with high probability.

HOT CARRIERS: OPPORTUNITIES AND CHALLENGES

Surface plasmons and localized plasmons, collective excitations of electrons near metal surfaces or in metal nanostructures, confine light down to tens of nanometers [1, 2], promising to bring photonics from the micro to the nano scale [3]. Plasmons rapidly decay to energetic hot carriers in the metal, which though a challenge for quantum plasmonics, proves useful as a nanoscale light capture technique for imaging [4], solar cells [5] and photochemical energy conversion systems [6, 7].

Plasmonic hot-carrier devices rely on extracting energetic carriers from the metal before they thermalize and lose their energy [8, 9]. Their efficiency can theoretically surpass conventional semiconductor devices [10], but remains an order of magnitude below theoretical limits in most applications [11–14]. This review briefly summarizes the mechanisms underlying hot carrier harvesting, and highlights ongoing efforts and open challenges to boost efficiency of hot carrier collection by using smaller plasmonic structures, finding new materials and by engineering interfaces.

DOWNSIZING FOR EFFICIENCY

Theoretical predictions using quantum-mechanical simulations of hot carrier generation and thermalization have played a vital role in illuminating their efficiency limits [15–17]. These simulations have sought to quantify the impact of nanostructure geometry, electromagnetic field distributions and metal electronic structure on the usable carrier energy and momentum distributions. Collectively, these studies identify several mechanisms and regimes depending on the material, photon frequency and size of the plasmonic structure.

Plasmonic hot carrier generation is predominantly plasmonically-enhanced photo-excitation of charge carriers in the metal. Close to plasmonic resonance, electromagnetic waves in free space couple strongly to the localized modes near the particle or surface structure and create a higher electric field intensity with a different spatial distribution than further away from resonance. Most importantly, generation of hot carriers depends on this electric field distribution and oscillation frequency, but not specifically (and directly) on whether the plasmon is off or on resonance.

The oscillating electric field within the metal can excite charge carriers in metals generating an initial energy distribution of hot carriers that depends on the electronic structure of the metal and the photon energy $\hbar\omega$. Figure 1(a) shows the initial carrier energy distribution in gold predicted from **first-principles calculations** (see glossary) of **direct transitions** and **indirect transitions** [17]. When the photon energy exceeds the **interband threshold** energy, the dominant process is direct excitation of electrons from a lower to higher band by absorbing a photon. In noble metals, such direct excitations leave a high energy hole in the d band of the metal and a lower energy electron near the Fermi level (the blue 'hills' in Fig. 1(a)). Below the interband threshold, in bulk metal or large nanostructures, the dominant process is phonon-assisted intraband absorption which excites charge carriers by absorbing a photon and additionally either absorbing or emitting a phonon. This indirect excitation generates a relatively flat energy distribution of both electrons and holes each ranging from zero to the photon energy, mostly independent of the metal (the red 'plateaus' in Fig. 1(a)).

The phonon is necessary in the indirect process to provide momentum to move the carrier from one state to another within the same band because the momentum of the absorbed photon is negligible compared to electrons. In nanostructures, this momentum may also be obtained from the surface of the material with non-negligible probability as the electron reflects off it. This 'geometry-assisted' intraband absorption, the focus of initial theories of plasmonic hot carrier generation [15, 16], coexists with the above mechanisms that depend more on material than nanostructure geometry. Intraband processes are less sensitive to the metal electronic structure and can be reasonably approximated by analytical free-electron and **jellium** models [18], but the interband processes depend sensitively on the joint density of states of the metal and require first-principles electronic structure calculations.

The rates of the above mechanisms are all proportional to the square of the electric field, and are therefore enhanced near plasmonic resonance when the localized field intensity

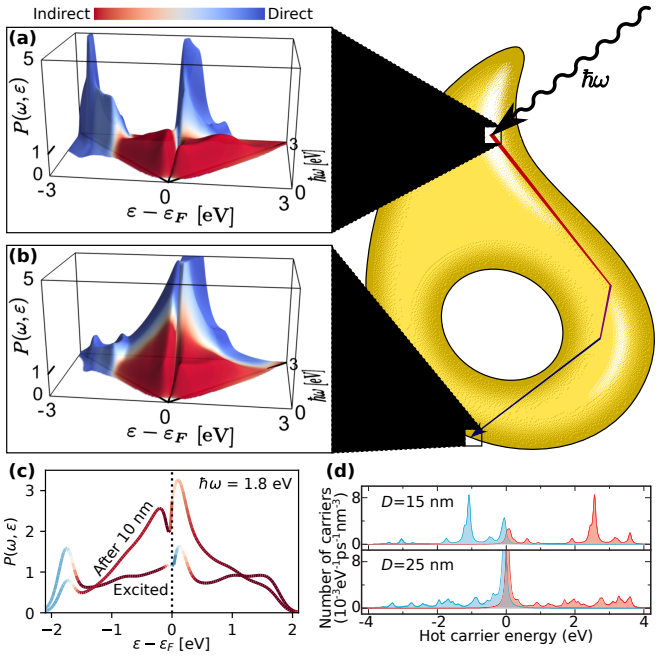

FIG. 1. **Predictions of generated and transported hot carrier distributions.** (a) Hot carrier distribution $P(\omega,\varepsilon)$ in gold as a function of photon energy $\hbar\omega$ and carrier energy ε immediately after plasmon decay [17], and (b) after transporting 10 nm through the metal, where most high energy carriers lose their energy to carriers closer to the Fermi level by electron-electron scattering [19]. (c) Comparison of (a) and (b) at a specific photon energy of 1.8 eV. (d) Jellium (free-electron) models predict increased generation of high-energy carriers in smaller nanoparticles [15]. (Adapted with permission from Ref. [17] (©2016, American Chemical Society), Ref. [19] (©2018, American Physical Society) and Ref. [15] (©2014, American Chemical Society).

is maximum. In large nanostructures, the electric field can vary substantially with position, leading to a spatial distribution of hot carriers within the structure as well. The initial energy distribution of carriers discussed so far (Fig. 1(a)) is generated with varying probability throughout the nanostructure. These carriers must then transport through the structure to reach a surface where they can be extracted. Note that the electric field of the plasmon affects the initial carrier distribution, but negligibly impacts the subsequent transport of carriers because of the high (Fermi) velocity of electrons in metals and the rapid oscillation frequency. Instead the dominant impact of carrier transport is energy and momentum relaxation due to electron-electron and electron-phonon scattering within the material [17, 19]. Figure 1(b) shows the energy distribution after transporting the carriers through 10 nm of gold: higher energy electrons and holes rapidly lose their energy primarily by electron-electron scattering to generate a greater number of lower energy carriers piling up near the Fermi energy (Figure 1(c)). This rapid energy relaxation during hot carrier transport is a key limiting factor in the efficiency of hot-carrier energy conversion processes.

Carrier transport is no longer an important consideration in metal nanoparticles smaller than the typical hot electron mean-free paths $\sim$ 10 nm (eg. for electrons $\sim$ 1 eV from the Fermi level in noble metals). In this regime, the particle size directly influences the hot carrier distribution because the geometry-assisted mechanism dominates carrier generation. Free-electron and jellium model simulations show that the carrier distributions are quite sensitive to the particle size: the probability of generating higher-energy carriers increases with decreasing particle size (Fig. 1(d)) [15]. In very small particles, the discreteness of energy states is an additional consideration that dramatically changes the distributions for small changes in size [16]. A quick estimate of the typical energy spacing is $E_F/(k_F R)$, where E_F is the Fermi energy, k_F the Fermi wavevector and R is the particle radius, amounting to 0.2 eV level spacing for 5 nm particles and 1 eV level spacing for 1 nm particles. Additionally, in such small particles, surfaces, interfaces and their defects play an increasingly important role due to the high surface-to-volume ratio. This results in significant variation from one particle to another in the ensemble, not captured in the theoretical models.

In summary, plasmonically-enhanced electric field distributions in metal nanostructures photo-excite carriers in the material, whose energy distributions are dependent primarily on the metal electronic structure (interband threshold and joint density of states), and whose spatial distribution is determined by the electric field profile. The hot carriers need to transport to the interface and cross into another material in order to be 'collected' for a detector or energy conversion application. We next discuss considerations for the plasmonic material and interface that respectively determine transport and collection limits to the efficiency of hot-carrier devices.

BEYOND NOBLE METALS

The most widely used plasmonic materials are the best conducting metals, including the noble metals (gold, silver and copper) and aluminum, in order to attain lower losses and higher plasmonic enhancement. Of these, gold has been used the most because of its relative stability in nanostructures, but its shallow d bands limit the surface plasmon resonance within the visible spectrum at about 2.8 eV [24]. Increasingly, experimental challenges due to surface oxidation in silver and aluminum have been addressed targeting lower loss and higher frequency applications extending to the ultraviolet range (about 3.6 eV and 6 eV respectively) [25, 26]. Without d bands, aluminum also exhibits qualitatively different carrier distributions - uniform electron and hole distributions even with direct excitations [27], and relaxation dynamics dominated by a stronger electron-phonon coupling [28]. For photochemical applications, and especially for the challenging carbon dioxide reduction reaction (CO2RR) [29], copper is gaining traction due to its higher catalytic activity [30] despite being lossier than gold with shallower d bands. Hot carriers generated in copper nanoparticles can both drive CO2RR directly [31], or in conjunction with single-atom active sites such as

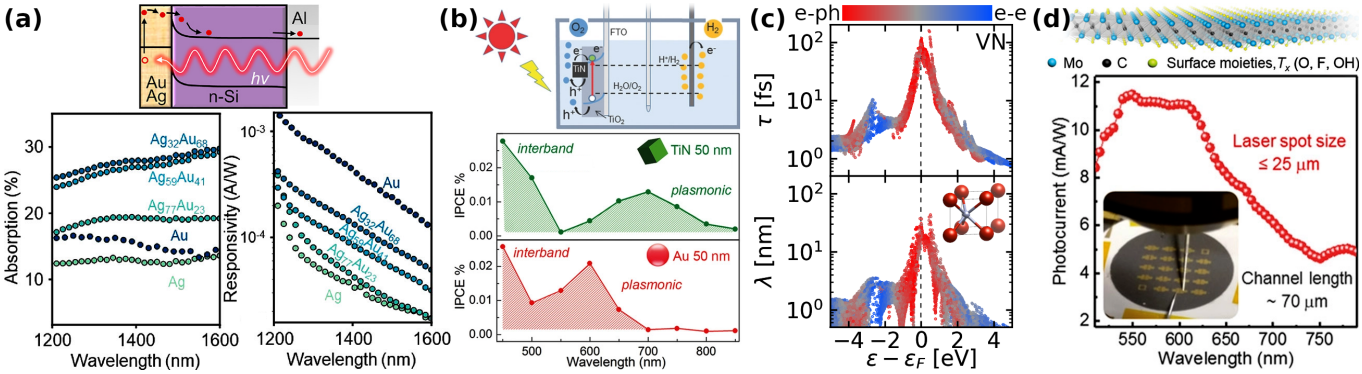

FIG. 2. **Materials beyond noble metals for plasmonic hot carrier collection.** (a) Gold-silver alloys exhibit tunable absorption that can surpass pure gold and silver, but fall short of gold on the photoresponsivity: collected hot carrier current per incident power [20]. (b) Transition metal nitrides such as titanium nitride can surpass gold in the incident photon to electron conversion efficiency (**IPCE**) due to broader band absorption and lower Schottky barriers to carrier collection [21]. (c) Carrier lifetimes in transition metal nitrides such as vanadium nitride can exceed those in noble metals, leading to comparable mean free paths despite the smaller Fermi velocities [22]. (d) Two-dimensional (2D) metallic ceramics, MXenes, combine the stability of ceramics like nitrides with the high plasmonic confinement of 2D plasmonic materials like graphene, and exhibit higher photoresponsivity and IPCE than both noble metals and 3D nitrides [23]. (Adapted with permission from Ref. [20] (©2020, American Chemical Society), Ref. [21] (©2017, Wiley-VCH), Ref. [22] (©2018, IOP Publishing) and Ref. [23] (©2019, Wiley-VCH).)

ruthenium that can lower reaction barriers further [32].

Going beyond elemental metals would be advantageous for flexibility in tuning both the plasmonic (optical) response and hot carrier distributions. While it is possible to shift plasmonic resonances by changing the dielectric constant of the surrounding dielectric medium [15], it would be advantageous to tune the resonance independently of the dielectric since that material choice is more tightly constrained for hot-carrier applications by interface considerations for hot carrier collection, as we discuss later.

The simplest material platform with tunable plasmonic resonance are alloys of noble metals, facilitating response ranging almost continuously from the lossier lower frequency plasmonics in gold to the lower-loss near-UV plasmonics in silver [33–36]. This tunability also exhibits potential for performance improvements in photocatalysis and photodetection [20, 37–40]. Fig. 2(a) [20] shows that absorption in the near-infrared (NIR) spectrum can be enhanced in Ag-Au alloy thin films compared to the pure metals. However, the **photoresponsivity**, which measures net hot carriers collected after excitation, is higher for pure Au than all the alloys, hypothesized to arise from increased carrier scattering in the alloys. Comprehensive first-principles prediction of energy relaxation of hot carriers in alloys accounting for scattering due to disorder, in addition to electron-phonon and electron-phonon processes [17], is now needed to build a detailed mechanistic picture analogous to the previous section for pure metals.

In addition to tunability, a key requirement for increased efficiency in plasmonic hot-carrier applications is reducing the size of the metal structure, as discussed in the previous section. This requires materials that remain stable at small dimensions, under illumination where they may undergo severe local heating, and potential in corrosive electrolytes for photochemical applications. Metallic ceramics such as transition metal nitrides, long applied as protective coatings to metals [41], have gained recent interest as plasmonic metals in their own right because of their outstanding ability to withstand extreme temperatures and harsh chemical environments, in addition to optical properties comparable to noble metals [42, 43]. These nitrides are also increasingly promising for harvesting hot carriers [44], with TiN in particular matching the optical response of gold closely, while being CMOS-compatible for integrating into semiconductor devices for hot-carrier photodetection [45]. TiN has also shown to be effective in photocatalytic applications [21, 46], outperforming the incident photon to electron conversion efficiency (IPCE) of gold for water-splitting using a TiO_2 nanowire catalyst (Fig. 2(b)) [21]. This increase in performance emerges from a broader plasmonic absorption band as well as a lowered Schottky barrier, allowing the non-zero IPCE to extend to longer wavelengths (lower frequencies). Theoretical predictions also confirm favorable hot carrier energy distributions and carrier transport lengths accounting for electron-phonon and electron-electron scattering in several transition metal nitrides compared to noble metals [22]. In particular, predicted carrier **lifetimes** in vanadium nitride are longer than noble metals, while the **mean free paths** remain similar to noble metals due to a lower Fermi velocity (Fig. 2(c)) [22].

Another avenue to simultaneously mitigate hot carrier transport issues and increase plasmonic enhancement is to use two-dimensional (2D) plasmonic materials. Graphene-based plasmonic structures can achieve **field enhancements** almost an order of magnitude larger than noble metals [47], but this performance is restricted to infrared frequencies. Similarly, while low-energy carriers can transport two orders of magnitude longer in graphene, carriers with 1 eV energy and greater, needed for most hot-carrier applications, have shorter mean free paths than in noble metals due to strong optical-phonon

scattering [48]. Theoretical calculations show that 2D metals, such as a single atomic layer of silver, 'argentene', could simultaneously extend the high **plasmonic confinement** of graphene to optical frequencies and retain carrier transport better than 3D metals to higher energies [49, 50]. However, there is no pathway yet to experimentally achieve such monolayers of elemental metals.

Once again, metallic ceramics come to the rescue! In particular, **MXenes**, the two-dimensional counterpart of MAX phases that are nitride or carbide compounds of transition metals, exhibit impressive optical properties [53] as well as promise for hot-carrier photodetection [23, 54, 55] and photocatalysis [56–59]. Figure 2(d) shows the performance of flexible thin-film photodetectors of carbide MXene material Mo_2CT_x, where T is a surface-terminating group [23]. The spectral response peaks in the visible range, with the measured photocurrent corresponds to an IPCE of $\sim 2\%$, which is one-two orders of magnitude greater than that of TiN, noble metals and their alloys in Fig. 2(a-b). Even so, there is significant room for increasing the fraction of photons converted to collected electrons from 2% towards 100%, allowing for further increase in sensitivity for photodetection with new materials and interfaces.

GETTING PAST THE SURFACE

Despite significant advances in materials for plasmonic hot carriers, a key challenge remains: low conversion of photons to collected carriers in most cases. Experiments have explored hot carrier separation across numerous interfaces of plasmonic metals, especially the noble metals, with semiconductors including silicon, TiO_2, CdSe and GaN [60]. Broadly, these experiments fall into two categories: direct photocurrent measurements of collected carriers across metal-semiconductor interfaces of large-area plasmonic nanostructures [51, 61–63], and indirect or transient detection of collected carriers from plasmonic nanoparticles, typically using ultrafast spectroscopy [64–66].

In larger nanostructures, the charge transfer across the metal-semiconductor interface is predominantly expected to proceed from carrier excitation within the metal, followed by transport and collection, as shown in Fig. 1. Energy relaxation during transport of carriers to the surface is the first bottleneck shown in Fig. 1(b), which can be mitigated by geometrical design to minimize carrier transport distances and by materials that facilitate transport of higher energy carriers. However, even if these carrier transport issues within the metal are addressed, a major limit to the efficiency is that most carriers that reach the surface reflect back into the metal [67]. This reflection occurs primarily because of momentum mismatch between metals with fast electrons near the Fermi level and semiconductors with much slower electrons near the band edges that cause most hot carriers to be reflected back into the metal, estimated for free electrons (parabolic bands) using the Fowler model [63]. Holes in the *d* bands of metals exhibit complex non-parabolic band structures with low velocities, and can thereby exhibit higher injection probabilities (extracted from measured photocurrents using theoretically predicted carrier distributions) than predicted by the Fowler model (Fig. 3(a)). Explaining this increased probability requires accounting for the momentum distribution of holes at each energy from a **DFT** electronic structure calculation, as well as for tunneling through the Schottky barrier [51], highlighting the need for first-principles quantum-mechanical treatment of interfacial hot-carrier transport.

Collection of hot carriers generated in the metal is therefore limited by energy loss during transport as well as reflection at the interface during injection prior to collection in a semiconductor (black lines in Fig. 3(b)). Instead, directly generating carriers at the interface, using charge transfer excitations that produce electrons and holes on opposite sides of the interface (blue lines in Fig. 3(b)), could theoretically eliminate both these losses. Experimental evidence for such plasmon-induced charge-transfer transitions (**PICTT**) is primarily from ultrafast spectroscopy of small metal nanoparticles on semiconductors [11, 68]. Such studies have identified material combinations with highly efficient charge collection, such as 40% electron injection from gold nanodots to TiO_2 completed within 240 fs of plasmon excitation [65], and 80% hole injection from 10-nm gold nanoparticles to GaN [66]. Ultrafast experiments have also detected energy transfer from metal hot carriers to semiconductor carriers, without a direct charge transfer across the interface [69]. However, high-efficiency charge collection, potentially exploiting interfacial transitions, is relatively rare in most metal-semiconductor interfaces and still predominantly restricted to ultrafast measurements involving small metal nanoparticles [70–73].

Quantum mechanical simulations of carrier dynamics at material interfaces could hold the key to understanding what makes certain material combinations most effective at charge collection. Most simulations of interfacial charge transfer processes adopt non-adiabatic molecular dynamics (**NAMD**) techniques, which approximately incorporate electronic transitions into DFT-based molecular dynamics simulations [74]. NAMD simulations show that charge density of plasmon modes on a metal atom cluster can decay into semiconductor conduction-band states (Fig. 3(c)), before relaxing back into the metal [52, 75]. Similar processes have been predicted in graphene on TiO_2 [76–78] and heterostructures of two-dimensional materials [79]. The efficacy of charge transfer strongly depends on the nanoparticle dimensions [80] and on its vibrational modes [81–83]. However, these simulations only include few tens of atoms of the metal, resulting in electronic states and vibrational modes rather different from electron bands and phonon modes of realistic nanoparticles. Additionally, these simulations treat atom motion classically, which is inaccurate below the Debye temperature and precludes phonon non-equilibrium effects such as phonon drag. Most importantly, efficient injection across large-area metal-semiconductor interfaces, rather than from small metal nanoparticles, remains an open challenge both theoretically

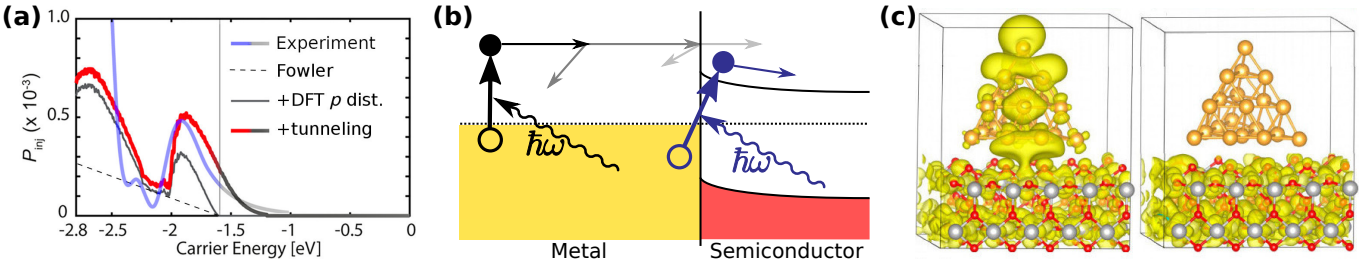

FIG. 3. **Getting hot carriers past the surface.** (a) Hole injection probability across Cu-GaN interface extracted from experiment using DFT-predicted carrier generation is underestimated by the classical Fowler model and requires accounting for the true hole momentum distribution from DFT and tunneling across the Schottky barrier. (b) Charge-transfer excitations across interfaces (blue lines) could bypass loss due to energy relaxation in transport and low injection efficiency at the interface (black lines). (c) Non-adiabatic molecular dynamics simulation of plasmon mode on 20-atom gold cluster decaying directly to electron in conduction band of TiO_2 (with hole in gold), before relaxing back to the metal. (Adapted with permission from Ref. [51] (©2020, American Chemical Society) and Ref. [52] (©2014, American Chemical Society).)

and experimentally.

CONCLUDING REMARKS

Plasmonic hot carriers have made great strides in the last decade, with an expanding materials toolkit spanning ceramics, especially transition metal nitrides that could enable stable plasmonic devices approaching the nanometer scale, and MXenes that additionally bring the higher confinement and field enhancement advantages of 2D plasmonics. With these advances, the typical photon to electron conversion efficiency has gradually increased from sub-percent to the few percent level. However, a significant gap remains between efficiency of collected current in large-area metal-semiconductor interfaces and the tens of percent efficiency in *transient* electron transfer probed using ultrafast spectroscopy.

The key challenge remains in getting carriers across the surface of the metal, where most carriers reflect back into the metal due to momentum mismatch with states outside the metal. Consequently, strategies to engineer the interfaces to break this momentum-matching bottleneck are of utmost importance. This could include geometrical approaches such as nanoscale roughening to break momentum conservation or new plasmonic materials such as ceramics whose lower carrier momenta are better matched with semiconductors. Additionally, these designed interfaces could support direct carrier separation across metal-semiconductor interfaces with higher probability, with the goal of bringing typical photocurrent extraction efficiency in line with the much higher charge transfer efficiencies so far primarily limited to transient measurements.

ACKNOWLEDGEMENTS

We thank support from the National Science Foundation under grant No. DMR-1956015. AH acknowledges support from the American Association of University Women (AAUW) fellowship.

HIGHLIGHTS

- New plasmonic materials such as transition metallic nitrides show promise for efficient hot carrier collection with stability at dimensions and environmental conditions out of reach for noble metals.
- Two-dimensional metallic ceramics such as MXenes may bring high confinement and field enhancement of 2D plasmonics to hot-carrier applications.
- Interfacial charge transfer excitations may lead to significant increase in efficiency by bypassing both carrier transport and interfacial injection losses.

OUTSTANDING QUESTIONS

- Transfer of hot carriers across metal-semiconductor interfaces remains a major bottleneck in photocurrent extraction efficiency: can new material combinations or interface modifications resolve the momentum mismatch between electronic states across the interface?
- Interfacial charge transfer excitations lead to high efficiency in transient measurements of select nanoparticle-semiconductor systems, but can this be made the dominant mechanism in photocurrent extraction from large-area metal-semiconductor plasmonic devices?
- First-principles electronic dynamics using non-adiabatic molecular dynamics (NAMD) simulations provide valuable insights into interfacial charge transfer and excitations, but how does one realistically account for phonon / vibrational effects in solid / nanoparticle interfaces given the system size limits of this method?

- What computational techniques will provide the right balance of computational cost and accuracy for first-principles design of material combinations and interfaces for efficient hot carrier transfer?

GLOSSARY

- **Density-functional theory (DFT)**: the most common approximate technique employed for quantum-mechanical simulations of the electronic structure of materials.
- **Direct transitions**: electronic excitations producing electrons and holes separated by the energy of an absorbed photon, and with equal momenta.
- **Field enhancement**: ratio of electric field in localized or surface plasmon mode compared to corresponding electromagnetic wave in free space, which is typically much greater than one as a direct consequence of plasmonic confinement.
- **First-principles calculations**: quantum-mechanical simulations of electrons that account for the crystal structure and detailed electronic band structure of materials. (See density-functional theory.)
- **Incident photon to electron conversion efficiency (IPCE)**: fraction of incident photons converted to electrons (or charge carriers including holes, more generally), collected as a photocurrent or used to drive a chemical reaction.
- **Indirect transitions**: electronic excitations that produce electrons and holes with different momenta, relying on additional interactions such as a phonon to provide momentum. (See Direct transitions.)
- **Interband threshold**: minimum photon energy at which a material supports direct transitions, requiring indirect transitions at smaller photon energies (longer wavelengths).
- **Jellium models**: quantum-mechanical calculations that ignore the crystal structure and detailed band structure, treating metals effectively as free-electron gases.
- **Lifetimes** (of carriers): average time for which photo-excited charge carriers retain their energy, typically limited by electron-electron and electron-phonon scattering processes in plasmonic metals and strongly dependent on the energy of the carrier.
- **Mean free path** (of carriers): average distance travelled by a photo-excited carrier before it scatters against other electrons or phonons to lose its energy and momentum, equal to the product of carrier's lifetime and velocity.
- **MXenes**: two-dimensional 'MAX-phase'-like materials, which are typically nitrides or carbides of transition metals with surface functional groups to stabilize the two-dimensional structure.
- **Non-adiabatic molecular dynamics (NAMD) simulations**: approximate first-principles technique to account for electron dynamics by introducing electronic transitions / excitations on top of DFT-based molecular dynamic solutions, which by themselves only account for motion of atoms with electrons in the ground state.
- **Photoresponsivity**: ratio of photocurrent to incident optical power, which measures the efficiency of converting photons to collected electrons. Multiply photoresponsivity (in A/W) by photon energy in eV to convert to IPCE.
- **Plasmonic confinement**: reduction in length scale over which electromagnetic fields are localized in plasmon modes compared to electromagnetic waves in free space.
- **Plasmon-induced charge-transfer transitions (PICTT)**: absorption of a photon at an interface to excite an electron from one side of the interface to the other, producing an electron-hole pair that is already separated between a metal and a semiconductor. This is in contrast to conventional plasmonic hot carrier processes that generate carriers in the metal that subsequently transport to and cross an interface.

---

[1] R. Heintzmann and M. G. L. Gustafsson, Nature Photon. **3**, 362 (2009).
[2] S. Kawata, Y. Inouye, and P. Verma, Nature Photon. **3**, 388 (2009).
[3] M. S. Tame, K. R. McEnery, S. K. Ozdemir, J. Lee, S. A. Maier, and M. S. Kim, Nature Phys. **9**, 329 (2013).
[4] P. J. Schuck, Nature Nanotech. **8**, 799 (2013).
[5] F. Wang and N. A. Melosh, Nano Lett. **11**, 5426 (2011).
[6] S. Mubeen, J. Lee, N. Singh, S. Kramer, G. D. Stucky, and M. Moskovits, Nature Nanotech. **8**, 247 (2013).
[7] S. Linic, P. Christopher, and D. B. Ingram, Nature Mater. **10**, 911 (2011).
[8] M. Moskovits, Nature Nanotech. **10**, 6 (2015).
[9] M. L. Brongersma, N. J. Halas, and P. Nordlander, Nature Nanotech. **10**, 25 (2015).
[10] C. Clavero, Nature Photon. **8**, 95 (2014).
[11] Y. Tian and T. Tatsuma, J. Am. Chem. Soc. **127**, 7632 (2005).
[12] Y. Nishijima, K. Ueno, Y. Yokota, K. Murakoshi, and H. Misawa, J. Phys. Chem. Lett. **1**, 2031 (2010).
[13] Y. Zhang, C. Yam, and G. C. Schatz, J. Phys. Chem. Lett. **7**, 1852 (2016).
[14] B. Zhao, I. Aravind, S. Yang, Y. Wang, R. Li, B. Zhang, Y. Wang, J. M. Dawlaty, and S. B. Cronin, J. Phys. Chem. C **125**, 6800 (2021).

[15] A. Manjavacas, J. G. Liu, V. Kulkarni, and P. Nordlander, ACS Nano **8**, 7630 (2014).

[16] H. Zhang and A. O. Govorov, J. Phys. Chem. C **118**, 7606 (2014).

[17] A. M. Brown, R. Sundararaman, P. Narang, W. A. Goddard III, and H. A. Atwater, ACS Nano **10**, 957 (2016).

[18] J. B. Khurgin, Nanophotonics **9**, 453 (2020).

[19] A. S. Jermyn, G. Tagliabue, H. A. Atwater, W. A. Goddard, P. Narang, and R. Sundararaman, Phys. Rev. Mater. **3**, 075201 (2019).

[20] L. J. Krayer, K. J. Palm, C. Gong, A. Torres, C. E. P. Villegas, A. R. Rocha, M. S. Leite, and J. N. Munday, ACS Photon. **7**, 1689 (2020).

[21] A. Naldoni, U. Guler, Z. Wang, M. Marelli, F. Malara, X. Meng, L. V. Besteiro, A. O. Govorov, A. V. Kildishev, A. Boltasseva, and V. M. Shalaev, Adv. Opt. Mater. **5**, 1601031.

[22] A. Habib, F. Florio, and R. Sundararaman, J. Opt. **20**, 064001 (2018).

[23] D. B. Velusamy, J. K. El-Demellawi, A. M. El-Zohry, A. Giugni, S. Lopatin, M. N. Hedhili, A. E. Mansour, E. D. Fabrizio, O. F. Mohammed, and H. N. Alshareef, Adv. Mater. **31**, 1807658 (2019).

[24] V. Amendola, R. Pilot, M. Frasconi, O. M. Maragò, and M. A. Iatì, J. Phys.: Conden. Matt. **29**, 203002 (2017).

[25] A. S. Baburin, A. M. Merzlikin, A. V. Baryshev, I. A. Ryzhikov, Y. V. Panfilov, and I. A. Rodionov, Opt. Mater. Express **9**, 611 (2019).

[26] C.-W. Cheng, S. S. Raja, C.-W. Chang, X.-Q. Zhang, P.-Y. Liu, Y.-H. Lee, C.-K. Shih, and S. Gwo, Nanophotonics **10**, 627 (2021).

[27] R. Sundararaman, P. Narang, A. S. Jermyn, W. A. Goddard III, and H. A. Atwater, Nature Commun. **5**, 12 (2014).

[28] M.-N. Su, C. J. Ciccarino, S. Kumar, P. D. Dongare, S. A. Hosseini Jebeli, D. Renard, Y. Zhang, B. Ostovar, W.-S. Chang, P. Nordlander, N. J. Halas, R. Sundararaman, P. Narang, and S. Link, Nano Lett. **19**, 3091 (2019).

[29] R. Li, W.-H. Cheng, M. H. Richter, J. S. DuChene, W. Tian, C. Li, and H. A. Atwater, ACS Energy Lett. **6**, 1849 (2021).

[30] Y. Xin, K. Yu, L. Zhang, Y. Yang, H. Yuan, H. Li, L. Wang, and J. Zeng, Adv. Mater. **n/a**, 2008145.

[31] J. S. DuChene, G. Tagliabue, A. J. Welch, X. Li, W.-H. Cheng, and H. A. Atwater, Nano Lett. **20**, 2348 (2020).

[32] L. Zhou, J. M. P. Martirez, J. Finzel, C. Zhang, D. F. Swearer, S. Tian, H. Robatjazi, M. Lou, L. Dong, L. Henderson, P. Christopher, E. A. Carter, P. Nordlander, and N. J. Halas, Nature Energy **5**, 61 (2020).

[33] X. López Lozano, C. Mottet, and H.-C. Weissker, J. Phys. Chem. C **117**, 3062 (2013).

[34] C. Gong and M. S. Leite, ACS Photon. **3**, 507 (2016).

[35] M. G. Blaber, M. D. Arnold, and M. J. Ford, J. Phys.: Cond. Matt. **22**, 143201 (2010).

[36] S. Link, Z. L. Wang, and M. A. El-Sayed, J. Phys. Chem. B **103**, 3529 (1999).

[37] L. Zhou, D. F. Swearer, C. Zhang, H. Robatjazi, H. Zhao, L. Henderson, L. Dong, P. Christopher, E. A. Carter, P. Nordlander, and N. J. Halas, **362**, 69 (2018).

[38] M. Valenti, A. Venugopal, D. Tordera, M. P. Jonsson, G. Biskos, A. Schmidt-Ott, and W. A. Smith, ACS Photon. **4**, 1146 (2017).

[39] S. K. F. Stofela, O. Kizilkaya, B. T. Diroll, T. R. Leite, M. M. Taheri, D. E. Willis, J. B. Baxter, W. A. Shelton, P. T. Sprunger, and K. M. McPeak, Adv. Mater. **32**, 1906478 (2020).

[40] C. chao Jian, J. Zhang, W. He, and X. Ma, Nano Energy **82**, 105763 (2021).

[41] E. Budke, J. Krempel-Hesse, H. Maidhof, and H. Schüssler, Surf. Coat. Tech. **112**, 108 (1999).

[42] U. Guler, A. Boltasseva, and V. M. Shalaev, Science **344**, 263 (2014).

[43] P. Patsalas, N. Kalfagiannis, S. Kassavetis, G. Abadias, D. V. Bellas, C. Lekka, and E. Lidorikis, Mater. Sci. Eng. R Rep. **123**, 1 (2018).

[44] S. Ishii, S. L. Shinde, W. Jevasuwan, N. Fukata, and T. Nagao, ACS Photon. **3**, 1552 (2016).

[45] J. Gosciniak, F. B. Atar, B. Corbett, and M. Rasras, Sci. Rep. **9**, 6048 (2019).

[46] C. Li, W. Yang, L. Liu, W. Sun, and Q. Li, RSC Adv. **6**, 72659 (2016).

[47] G. X. Ni, A. S. McLeod, Z. Sun, L. Wang, L. Xiong, K. W. Post, S. S. Sunku, B.-Y. Jiang, J. Hone, C. R. Dean, M. M. Fogler, and D. N. Basov, Nature **557**, 530 (2018).

[48] P. Narang, L. Zhao, S. Claybrook, and R. Sundararaman, Adv. Opt. Mater. **5**, 1600914 (2017).

[49] R. Sundararaman, T. Christensen, Y. Ping, N. Rivera, J. D. Joannopoulos, M. Soljačić, and P. Narang, Phys. Rev. Mater. **4**, 074011 (2020).

[50] A. R. Echarri, J. D. Cox, and F. J. G. de Abajo, Optica **6**, 630 (2019).

[51] G. Tagliabue, J. S. DuChene, A. Habib, R. Sundararaman, and H. A. Atwater, ACS Nano **14**, 5788 (2020).

[52] R. Long and O. V. Prezhdo, J. Am. Chem. Soc. **136**, 4343 (2014).

[53] K. Hantanasirisakul and Y. Gogotsi, Adv. Mater. **30**, 1804779 (2018).

[54] J. Jeon, H. Choi, S. Choi, J.-H. Park, B. H. Lee, E. Hwang, and S. Lee, Adv. Func. Mater. **29**, 1905384 (2019).

[55] W. Li and J. G. Valentine, Nanophotonics **6**, 177 (2017).

[56] Z. Zhang, X. Jiang, B. Liu, L. Guo, N. Lu, L. Wang, J. Huang, K. Liu, and B. Dong, Adv. Mater. **30**, 1705221 (2018).

[57] Z. Lou, P. Zhang, J. Li, X. Yang, B. Huang, and B. Li, Adv. Func. Mater. **29**, 1808696 (2019).

[58] S. Ishii, S. L. Shinde, and T. Nagao, Adv. Opt. Mater. **7**, 1800603 (2019).

[59] S. Li, P. Miao, Y. Zhang, J. Wu, B. Zhang, Y. Du, X. Han, J. Sun, and P. Xu, Adv. Mater. **n/a**, 2000086 (2020).

[60] C. Clavero, Nature Photon. **8**, 95 (2014).

[61] S.-H. Lee, S. W. Lee, T. Oh, S. H. Petrosko, C. A. Mirkin, and J.-W. Jang, Nano Lett. **18**, 109 (2017).

[62] H. Nishi and T. Tatsuma, J. Phys. Chem. C **122**, 2330 (2018).

[63] G. Tagliabue, A. Jermyn, R. Sundararaman, A. Welch, J. DuChene, R. Pala, A. Davoyan, P. Narang, and H. Atwater, Nature Commun. **9**, 3394 (2018).

[64] Y. Tian and T. Tatsuma, J. Am. Chem. Soc. **127**, 7632 (2005).

[65] A. Furube, L. Du, K. Hara, R. Katoh, and M. Tachiya, J. Am. Chem. Soc. **129**, 14852 (2007).

[66] G. Tagliabue, J. S. DuChene, M. Abdellah, A. Habib, D. J. Gosztola, Y. Hattori, W.-H. Cheng, K. Zheng, S. E. Canton, R. Sundararaman, J. Sá, and H. A. Atwater, Nature Mater. **19**, 1312 (2020).

[67] H. Chalabi, D. Schoen, and M. L. Brongersma, Nano Lett. **14**, 1374 (2014).

[68] A. Furube and S. Hashimoto, NPG Asia Mater. **9**, e454 (2017).

[69] J. A. Tomko, E. L. Runnerstrom, Y.-S. Wang, W. Chu, J. R. Nolen, D. H. Olson, K. P. Kelley, A. Cleri, J. Nordlander, J. D. Caldwell, O. V. Prezhdo, J.-P. Maria, and P. E. Hopkins, Nature Nanotech. **16**, 47 (2021).

[70] K. Wu, J. Chen, J. R. McBride, and T. Lian, Science **349**, 632 (2015).

[71] S. Tan, A. Argondizzo, J. Ren, L. Liu, J. Zhao, and H. Petek, Nature Photon. **11**, 806 (2017).

[72] S. Tan, Y. Dai, S. Zhang, L. Liu, J. Zhao, and H. Petek, Phys. Rev. Lett. **120**, 126801 (2018).
[73] J. S. DuChene, B. C. Sweeny, A. C. Johnston-Peck, D. Su, E. A. Stach, and W. D. Wei, Angew. Chemie Int. Ed. **53**, 7887 (2014).
[74] L. Wang, R. Long, and O. V. Prezhdo, Ann. Rev. Phys. Chem. **66**, 549 (2015).
[75] T.-F. Lu, Y.-S. Wang, J. A. Tomko, P. E. Hopkins, H.-X. Zhang, and O. V. Prezhdo, J. Phys. Chem. Lett. **11**, 1419 (2020).
[76] R. Long, N. J. English, and O. V. Prezhdo, J. Am. Chem. Soc. **134**, 14238 (2012).
[77] Y. Wei, L. Li, W. Fang, R. Long, and O. V. Prezhdo, Nano Lett. **17**, 4038 (2017).
[78] R. Long, D. Casanova, W.-H. Fang, and O. V. Prezhdo, J. Am. Chem. Soc. **139**, 2619 (2017).
[79] L. Li, R. Long, and O. V. Prezhdo, Chem. Mater. **29**, 2466 (2016).
[80] D. N. Tafen, R. Long, and O. V. Prezhdo, Nano Lett. **14**, 1790 (2014).
[81] H. Wang, J. Bang, Y. Sun, L. Liang, D. West, V. Meunier, and S. Zhang, Nature Commun. **7**, 11504 (2016).
[82] Q. Zheng, Y. Xie, Z. Lan, O. V. Prezhdo, W. A. Saidi, and J. Zhao, Phys. Rev. B **97**, 205417 (2018).
[83] Z. Ji, H. Hong, J. Zhang, Q. Zhang, W. Huang, T. Cao, R. Qiao, C. Liu, J. Liang, C. Jin, L. Jiao, K. Shi, S. Meng, and K. Liu, ACS Nano **11**, 12020 (2017).